Metal-InP(110) interface properties: Temperature, dopant-concentration, and cluster-deposition dependencies

I. M. Vitomirov, C. M. Aldao, G. D. Waddill, C. Capasso, and J. H. Weaver
Department of Chemical Engineering and Materials Science, University of Minnesota, Minneapolis, Minnesota 55455
(Received 20 November 1989)

Synchrotron-radiation photoemission has been used to investigate the movement of the surface Fermi level, E_F, in the gap as a function of temperature, bulk dopant concentration, and the technique of interface formation for Ag/InP(110) and Ti/InP(110). Studies involving atom deposition at 300 and 60 K reveal temperature-independent substrate disruption with substrate retreat that is estimated to be ~4.4 monolayers (ML) for Ti and ~1 ML for Ag deposition. Atom distributions differ, however, because In atoms released by substrate disruption are kinetically trapped near the interface at 60 K but they are distributed in and atop the metal overlayer at 300 K. Moreover, Ag deposition at 60 K produces uniform overlayers because of restricted surface mobility whereas Ag clustering occurs for atom deposition at 300 K. Despite these significant differences in interface chemistry and morphology, both overlayers induce very different amounts of band bending at 60 K than at 300 K for n-type InP(110) doped at 4×10^{17} cm^{-3}. This temperature-dependent difference in band bending is significantly smaller for n- and p-type InP(110) doped at 2.5×10^{18} cm^{-3}. At higher coverage above the metallization threshold, the Schottky-barrier height is largely independent of substrate dopant concentration or measurement temperature but exhibits metal-specific values for Ag and Ti overlayers. The relationship between E_F movement and the details of interfacial bonding and morphology has been further examined by depositing preformed Ag clusters (rather than atoms) on pristine InP(110) surfaces. For cluster deposition, there was no noticeable substrate disruption and the Fermi-level position was not dependent on the size or number of clusters. This indicates that changes in surface relaxation under and around the clusters introduce states that determine band bending.

INTRODUCTION

Few areas of solid-state physics have offered as many controversies as that associated with Schottky-barrier development. To a large extent, this is because of the complex morphological and electronic structures of metal-semiconductor interfaces. Much of the research effort in the field has been focused on identification of interfacial properties controlling surface Fermi-level (E_F) movement.[1-9] Two models have attracted special attention, one emphasizing the role of substrate imperfections (e.g., vacancies, antisite defects)[3] and the other relating E_F movement to the tailing of metallic wave functions of the overlayer into the semiconductor.[4] While both approaches have enjoyed some success, their generality has come under increased scrutiny.

Recent temperature- and dopant-concentration-dependent studies of a number of metal-GaAs(110) interfaces[5-7] have shown that band bending varies approximately linearly with temperature T for submonolayer metal coverages on lightly doped substrates (~10^{17} cm^{-3}). Thermal cycling in the range 20 K $\leq T \leq$ 350 K showed that E_F movement was reversible when temperature-associated morphology changes were absent.[6] The temperature dependence was significantly diminished for heavily doped substrates but was still reversible. These same studies revealed symmetry in E_F movement for n- and p-GaAs type of the same dopant concentration, $N=N_D=N_A$. Explanation for the effects of substrate dopant concentration and temperature was provided by the dynamic coupling model (DCM).[7] This model assumed that the surface and the bulk of the semiconductor were in equilibrium, and it associated the Fermi-level position in the submonolayer regime with the coupling between adatom-derived states in the gap at the surface with bulk states of the majority carrier band outside the depletion region. The filling or spectral density of these new hybrid states depends on the wave-function overlap involving the bulk and adatom-induced states. This coupling is sensitive to changes in substrate doping and temperature because N determines the width of the depletion region (the barrier width) and T determines the distribution of carriers near the conduction-band minimum (CBM) or valence-band maximum (VBM).[5-7] An alternate picture, proposed by Hecht,[8] assumed that the surface was not in equilibrium with the bulk because of a surface photovoltage effect. The magnitude of the effect would carry the same dependence on N and T as that developed by Aldao *et al.*, and it would again emphasize the coupling of the surface with the bulk. Analysis of photon- and electron-flux-dependent movement of E_F as a function of N and T showed that the nonequilibrium component dominated.[9]

This paper focuses on N- and T-dependent E_F movement for metal-InP(110) interfaces. These metal-InP systems provide an important testing ground in the high-

 ©1990 The American Physical Society

coverage regime for the various Schottky-barrier models because of the relatively large separation between the predicted pinning positions of defects[3] (0.95 eV above the VBM) and metal-induced gap states (MIGS)[4] (0.76 eV above the VBM). In the low-coverage regime, they offer an opportunity to test the generality of the temperature- and dopant-concentration-dependent results observed for GaAs(110)-based interfaces. Indeed, relatively few studies have investigated temperature effects for InP interfaces,[3,10,11] and none has considered the effects of substrate dopant concentration.

In the following we show that very similar E_F movement is induced by weakly reactive Ag and strongly reactive Ti adatoms deposited onto InP(110). The high-coverage pinning positions are largely insensitive to system temperature, but they differ for Ag and Ti. Temperature profoundly affects the overlayer morphology for Ag because spontaneous clustering occurs at 300 K but not at 60 K. For Ti, strong interface reaction and uniform substrate coverage are observed to be independent of temperature. Detailed analysis demonstrates that temperature does not alter the amount of substrate atoms released into overlayer via substrate disruption. While the released In atoms are segregated to the metal surface for 300-K deposition, movement toward the free surface is kinetically inhibited at 60 K. The very similar E_F movement for Ag and Ti depositions indicates that this movement is not strongly correlated with the extent of substrate disruption or detailed interface geometry. Importantly, the Fermi-level movement exhibits the same dependence on T and N as for GaAs(110).

Finally, we demonstrate that the deposition method itself can significantly alter both the details of bonding across the interface and the surface Fermi-level position. This is done by comparing results obtained following conventional atom deposition with those obtained when preformed Ag clusters are deposited onto the InP(110) surface. These metallic clusters are formed in and on a condensed Xe buffer layer at 60 K. They are brought in contact with the InP(110) surface when the Xe buffer is desorbed. For Ag clusters, the resulting morphology is similar to that obtained for atom deposition at 300 K because there is spontaneous Ag clustering on the surface at 300 K. Cluster depositions, however, do not produce the InP(110) substrate disruption observed for atom deposition at 300 or 60 K. They do, however, alter surface relaxation in the vicinity of clusters. We postulate that the unique, coverage-insensitive E_F positions observed for the Ag(clusters)/InP(110) interfaces can be attributed to pinning by the electrically active states introduced into the gap by these changes in surface structure.[12]

EXPERIMENTAL PROCEDURES

Synchrotron-radiation photoemission experiments were performed at the University of Wisconsin Synchrotron Radiation Center (Stoughton, WI) using the Minnesota–Argonne–Los Alamos Extended Range Grasshopper monochromator and beamline. Photoelectrons were collected with a double-pass cylindrical mirror analyzer in a system with $\sim 5\times10^{-11}$ Torr operating pressure. Spectra recorded for each metal deposition included In $4d$ taken at $h\nu=40$ and 60 eV, P $2p$ taken at 140 and 170 eV, and valence-band emission taken at 60 eV. These choices of incident photon energies resulted in photoelectron mean free paths λ of ~ 4 and ~ 10 Å.[11] Melt-grown n-type (Sn doped at 4×10^{17} cm^{-3} and S doped at 2.7×10^{18} cm^{-3}) and p-type (Zn doped at 2.3×10^{18} cm^{-3}) InP purchased from Crystacomm Inc. was oriented and cut into posts $\sim 4\times4\times20$ mm^3. (The specified dopant concentrations represent the middle of the manufacturer's quoted range.) Mirror-like (110) surfaces were obtained by cleaving these posts *in situ* at 300 K. The microscopic surface quality was assessed using core-level and valence-band spectra. Partially pinned cleaves with E_F positions more than 60 meV from the band edge were discarded; this pinning was assessed at 300 K because partially pinned surfaces can appear unpinned at low temperature.[6,7] Measurements for clean surfaces indicated average E_F separation between n- and p-type In(110) of 1.39 and 1.31 eV at 60 and 300 K, respectively (bulk gap 1.42 and 1.35 eV).

Ag and Ti atom depositions were carried out at pressures less than 4×10^{-10} Torr using resistively heated W boats. The source-to-sample distance was 35 cm. The amount of deposited metal was monitored by a quartz crystal microbalance. One monolayer (ML) corresponds to 8.2×10^{14} atoms/cm^2, and conversion to angstrom units yields 1.45 Å/ML for Ti and 1.41 Å/ML for Ag. Monolayer units are chosen for convenience but do not imply epitaxial growth for either metal. Sample temperatures of 60 K were maintained by attaching a sample to a copper cold finger in contact with a closed-cycle He refrigerator.[5] The temperature, measured with a Si diode mounted on the cold finger, was maintained within 5 K of the desired value.

Ag cluster depositions were accomplished by first condensing 200 L of xenon (1 L$=10^{-6}$ Torr sec) to produce $\sim$30-Å-thick Xe buffer layers. Earlier experiments involving adsorption and desorption of Xe on GaAs(110) and InP(110) showed that the Xe layer itself did not induce any surface Fermi-level movement. Metal depositions onto the Xe buffer layer led to cluster formation on and probably within the Xe matrix. The Xe layer was desorbed when the sample was detached from the cold finger and warmed above $\sim$90 K and the preformed metal clusters were thereby lowered to the surface. The chance of sample contamination during warming was minimized by additional pumping provided with a turbomolecular pump, and the continuous operation of the refrigerator precluded Xe desorption from surfaces other than the sample itself. A complete set of substrate energy-distribution curves (EDC's) was taken after the system returned to base pressure. This procedure, starting from the cleaving and characterizing of a fresh surface, was repeated for each cluster coverage; it should not be confused with standard procedures of sequential atom-by-atom depositions onto a single surface.

INTERFACE MORPHOLOGY

Ag/InP(110) atom deposition

Figure 1 summarizes the In $4d$ core-level evolution for Ag/InP interfaces formed at 300 and 60 K by atom depo-

sition. These representative EDC's are normalized to the same height to emphasize line-shape changes. Electrostatic (band-bending) effects have been removed by aligning the substrate core-level feature. Except for phonon broadening, the clean-surface spectra show no change between 300 K (left) and 60 K (right). They are decomposed into the substrate bulk emission (1) and the surface-shifted component (2). The latter corresponds to semiconductor atoms at the relaxed free surface. The surface component contributes ~40% of the clean-surface emission at $h\nu=40$ eV for our collection geometry, and this yields an approximate electron mean free path of 4.1 Å. For Ag deposition at 300 K, the surface-shifted component remains for the full range of investigated coverages ($0.01 \leq \theta \leq 15$ ML) at the same relative binding energy (0.30 ± 0.03 eV) as measured at the clean surface. The surface-to-bulk emission intensity ratio (S/B) is initially reduced by Ag deposition, but it remains unchanged at coverages beyond ~3 ML. These results indicate that the Ag overlayer formed at 300 K clusters spontaneously and that there is incomplete substrate covering. Numerous studies of Ag overlayers on other semiconductors have indeed revealed a strong tendency for clustering at 300 K.[12–16] At the same time, Ag atom deposition gives rise to a new component (3) due to substrate disruption. This is not observed for other systems, and it will be discussed below.

Clear evidence for the overlayer clustering is provided by the logarithmic attenuation plots of Fig. 2. In the upper panel we show the changes in the component-specific and the total emission intensities for In 4d as a function of Ag coverage at 300 K. The results reveal nearly identical attenuation rates for the substrate and surface-shifted components. (Bulk and surface-shifted components attenuate with $1/e$ lengths of ~13 Å for $\theta_{Ag} \geq 4$ ML.) This slow decay of the substrate and surface emission indicates formation of a clustered overlayer since a uniform overlayer would reduce substrate emission with a $1/e$ decay length equal to the photoelectron mean free path of ~3.5 Å. The third component in the

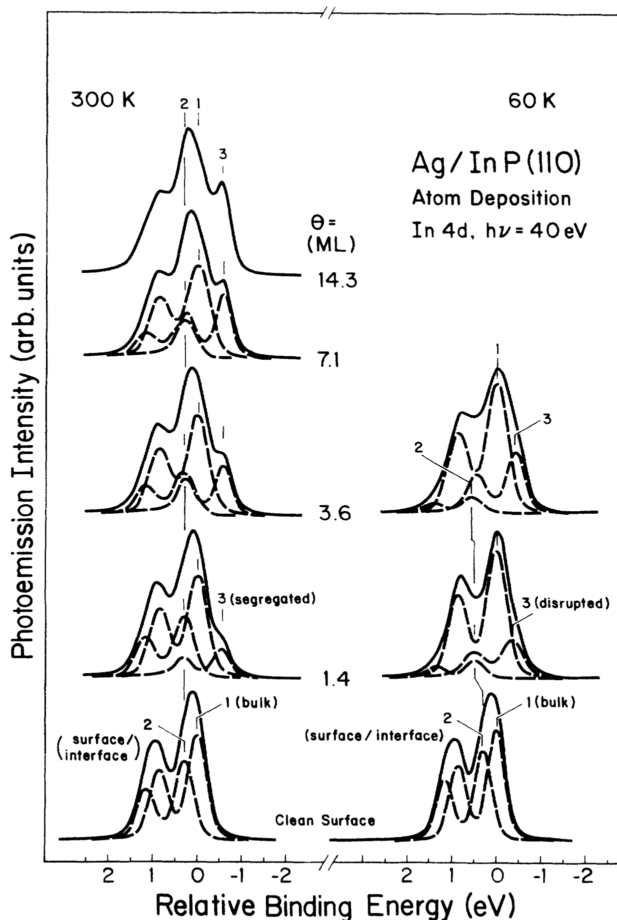

FIG. 1. Representative In 4d core-level EDC's and line-shape decompositions for 300- and 60-K atom deposition of Ag. Components 1 and 2 correspond to emission from bulk and surface atoms, respectively. Component 3 corresponds to In atoms released from the substrate and indicates equal amounts of substrate disruption at 300 and 60 K.

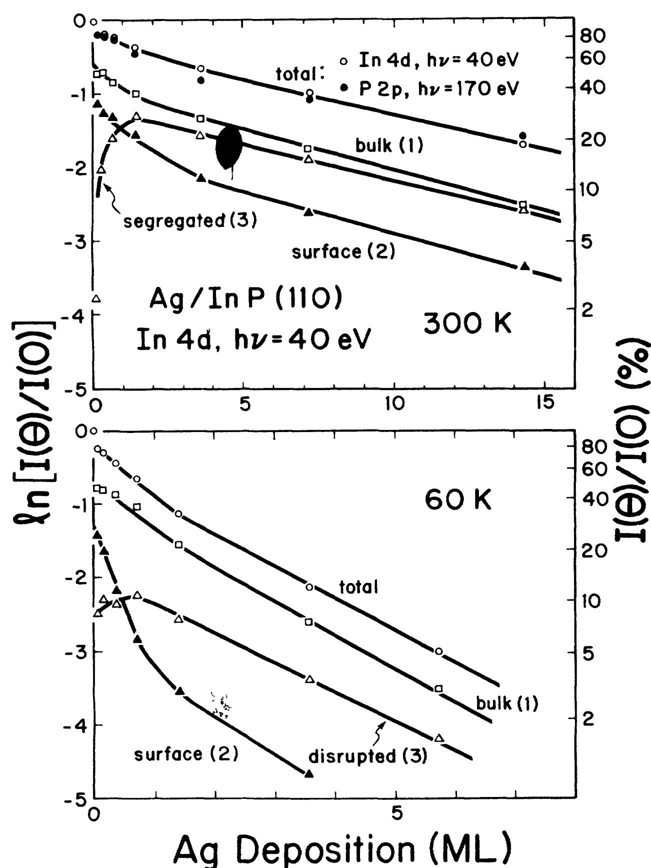

FIG. 2. Logarithmic core-level emission attenuations for 300-K (top) and 60-K (bottom) atom depositions of Ag. Note the factor-of-2 difference in the horizontal scales for the 300- and 60-K results. Gradual attenuation of the substrate signal at 300 K indicates overlayer clustering, whereas at 60 K the overlayer grows uniformly. To estimate the scale of In segregation for clustered overlayer at 300 K, component-3 intensity has been renormalized to the covered portion of the surface. Such renormalization reveals pronounced segregation of In atoms at 300 K and their kinetic trapping at 60 K.

attenuation plots (discussed below) corresponds to the In atoms released from the substrate.

A very different overlayer morphology is observed for interfaces formed by Ag atom deposition at 60 K. As shown in Fig. 1, the In $4d$ S/B ratio is much more rapidly reduced at 60 K than at 300 K and the surface component exhibits a definite shift to higher binding energy. This shift, emphasized by the vertical guides to the eye in Fig. 1 (right), saturates at -0.56 eV for $\theta_{Ag}=3.6$ ML and yields a slight shoulder on the high-binding-energy side of the 60-K spectra. Since this new component is attenuated at the same rate as the substrate above ~ 1.4 ML (see bottom panel of Fig. 2), we associate it with In atoms in the transition layer between the substrate and the Ag overlayer. It is analogous to the surface-shifted component, but reflects a change in the local bonding due to the immediate proximity of Ag atoms. The equivalent transition from the surface to the interface component is not evident in the 300-K spectra because the clusters are relatively large and they attenuate the emission from beneath them (a simple hemispherical cluster model[17] gives an estimated cluster radius of ~ 10 Å at 4 ML with $\sim 95\%$ of surface covered). Observation of this interfacial component at 300 K is further frustrated because of the near degeneracy with the much stronger surface-shifted component. Based on these line-shape considerations and the substrate emission attenuation shown in the lower panel of Fig. 2 ($1/e$ length of ~ 2.4 ML or 3.5 Å), we conclude that the interface formed at 60 K is uniformly covered for θ_{Ag} above ~ 1.4 ML. This reflects the drastically reduced Ag surface mobility at 60 K. This interface morphology is metastable with respect to changes in temperature and results of interface annealing to 300 K (not shown) reveal spontaneous clustering of the Ag overlayer (see Ref. 6 for such results for Ag/GaAs).

The line-shape decompositions shown in Fig. 1 also provide valuable information regarding the temperature dependence of adatom-induced substrate disruption (see Ref. 10 for a detailed discussion of the fitting procedures). It was recently suggested that Ag/InP(110) presents a rather unique system in which interface reactivity and defect formation are severely reduced at low temperature.[3] Our results unequivocally show that disruption does occur even at 60 K. In particular, disruption can be monitored through component 3 in Fig. 1, which corresponds to In atoms released from the substrate into the overlayer. At 300 K, component 3 is clearly resolved as a pronounced shoulder on the low-binding-energy side of the substrate emission. It is not as obvious to the eye in the 60-K spectra because of its smaller binding-energy shift of -0.39 eV compared to -0.54 eV for 300 K. We emphasize, however, that the fitting of the In $4d$ emission for 60-K deposition requires this third spin-orbit doublet, and fittings with deliberate omission of it resulted in unphysical broadening of the substrate Gaussian width. The observed difference in the relative binding energy is interesting and can be understood in terms of the different local environments of liberated In atoms. At 60 K, In outdiffusion is kinetically limited, and the In concentration (trapped) in the Ag overlayer is much higher than at 300 K where the kinetic constraints are removed and the In atoms are expelled at the free surface. Indeed, many previous studies have established that dissolution of segregated cations in metallic overlayers leads to the gradual decrease in the binding energy of their core electrons, and the increased shift of the disrupted component for Ag/InP(110) at 300 K agrees with this trend.[18,19]

In order to quantitatively estimate the amount of substrate disruption and cation release, it is instructive to follow the emission intensity of component 3. For the 300-K results, the signal intensity of the released In atoms has been normalized to the portion of the surface covered by Ag clusters. This procedure is motivated by the fact that In atoms segregate only from beneath the clusters and the remainder of the surface is still pristine InP. It thereby provides a more realistic indication of atomic distribution at heterogeneous interfaces and enables their comparison to systems presenting a layered growth mode. As shown in Fig. 2, the signal intensity of component 3 rises until $\theta_{Ag}\sim 1.5$ ML and is then gradually attenuated ($1/e$ length ~ 12 ML). This decay length is significantly shorter than the photoelectron mean free path in silver (~ 2.4 ML, as determined from the substrate attenuation at 60 K), and it reflects pronounced segregation to the surface of the Ag cluster of In atoms from the substrate. At 60 K, however, component-3 emission reaches its maximum at $\theta_{Ag}\sim 1$ ML. Thereafter, it decays at approximately the same rate as the substrate. This behavior reflects kinetic trapping of released In atoms at the interface at 60 K.

Comparison of the component-specific attenuation profiles of Fig. 2 clearly indicates that atom deposition at 300 K results in a much greater number of liberated In atoms within the photoemission probe depth than deposition at 60 K. In particular, the maximum renormalized signal intensity from these atoms (component 3) reaches $\sim 30\%$ at 300 K, compared to $\sim 10\%$ at 60 K. The processes causing substrate disruption, such as the release of energy associated with condensation and the energy gained by adatom-adatom bonding, do not depend on substrate temperature.[11] Indeed, the disrupted component signal increases very rapidly for submonolayer coverages at both 60 and 300 K, consistent with the same tendency toward disruption and defect formation at these temperatures. The difference in the component-3 maximum emission is then primarily due to kinetic constraints limiting In expulsion at reduced temperature. One should also note the importance of correctly normalized component-specific attenuation for quantitative assessment of outdiffusion of the released substrate atoms. As shown by line-shape decomposition of Fig. 1, the ratio of the disrupted to substrate component emission at each coverage is identical at 60 and 300 K for $\theta_{Ag}\leq 8$ ML. The core-level line shapes alone could then be misleading because of pronounced overlayer clustering at 300 K. This artifact is readily removed by monitoring simultaneous changes in the component-specific emission intensities and, for an inhomogeneous overlayer, by normalizing the emission of the outdiffused substrate species to the covered portion of the surface.

In summary, we have established that Ag/InP interfaces formed by atom deposition exhibit limited substrate

disruption at 300 and 60 K. At 300 K, spontaneous clustering of Ag adatoms results in a heterogeneous interface with significant numbers of liberated cations. Based on the cation attenuation, we conclude that these released In atoms are expelled to the free surface of the Ag clusters. Calculations based on bulk thermodynamics yield a small negative heat of solution of In in Ag matrix (-6.7 kJ/mole) indicative of a weak tendency for intermixing.[20] These calculations, however, are of limited value in estimating actual preferential location of the released In atoms in a heterogeneous Ag overlayer having a constantly evolving distribution of cluster sizes. Following more elaborate calculations of cohesive and atomic energies, Weaver *et al.*[21] predicted In segregation at this interface. Intriguingly, P $2p$ EDC's do not show any disruption-induced feature at either temperature. The P $2p$ emission is attenuated similar to the In $4d$ emission and indicates that disrupted P atoms from the substrate are also segregated to the free surface of Ag clusters at 300 K, in agreement with the segregation trends predicted in Ref. 21. The lack of any change in the P $2p$ core-level line shape is then attributed to the degeneracy in the P $2p$ binding energy between the substrate atoms and atoms released in the overlayer. At 60 K, liberated substrate atoms are kinetically trapped at the interface, and no evidence for segregation is found. Reduced temperature also quenches adatom surface mobility and results in nearly uniform overlayer growth.

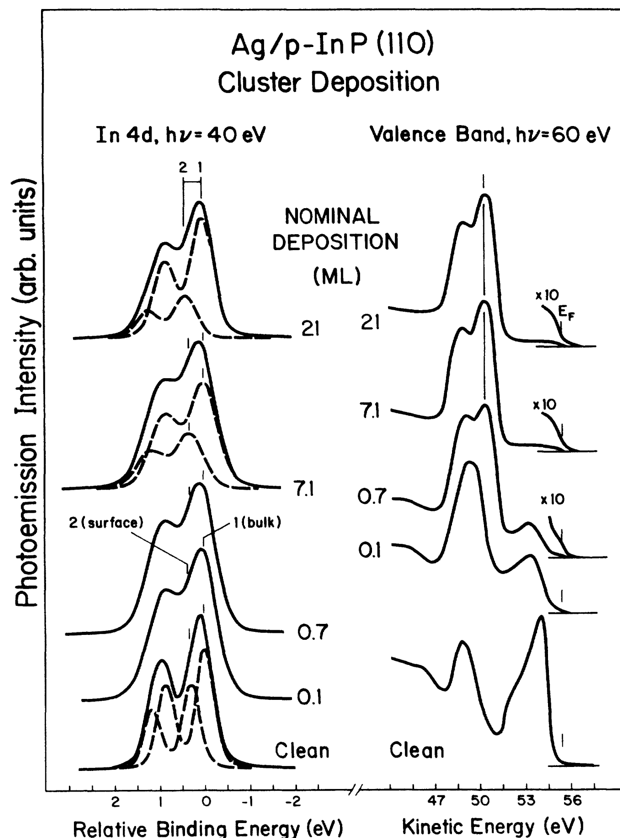

FIG. 3. Representative In $4d$ core-level spectra (left) and valence-band spectra (right) for Ag cluster deposition. In $4d$ line-shape decompositions show decrease in the relative intensity of the surface component caused by cluster-induced loss of surface relaxation. These spectra do not reveal any surface disruption. Valence bands show Fermi-level cutoff and development of the full Ag d-band width at 0.7 ML, indicative of the metallic character of the overlayer.

Ag/InP(110) cluster deposition

In the left panel of Fig. 3, we show In $4d$ energy-distribution curves (EDC's) for the Ag/InP(110) interface formed by cluster deposition. The clean-surface spectra were obtained at 60 K and those following cluster deposition at ~ 120 K. Spectra presented in Fig. 3 for representative Ag depositions stand in sharp contrast with those for atom-by-atom deposition because they exhibit no new Ag-induced features (such as feature 3 in Fig. 1). The only changes in the In $4d$ EDC's from the clean surface as the Ag deposition is increased are Gaussian line-shape broadening and a reduction of the S/B ratio. The spectral broadening is related in part to phonon contributions because the clean spectra were taken at 60 K and spectra following Xe desorption were taken at ~ 120 K. Even greater broadening arises from inhomogeneous band bending expected at low coverages. The relative loss of the surface component is due to cluster-induced changes in the surface geometry around the cluster perimeter as well as beneath the clusters. In particular, spectra obtained for $h\nu = 40$ eV and our collection geometry showed a S/B ratio of 0.52 and 0.36 at ~ 7 and 21 ML, respectively, as compared to 0.65 for the cleaved surface. These regions of unrelaxed surface are caused by interfacial strain at the cluster-semiconductor contact that, as we argue later, probably plays a substantial role in Fermi-level movement. Equivalent results concerning surface component attenuation were obtained from the P $2p$ spectra (not shown). They are in agreement with a wealth of data for metal(clusters)/GaAs(110) interfaces, as well as Ga(clusters) and Au(clusters)/InP(110) interfaces.[11,12,17]

Insight into the geometry of these interfaces formed by metal cluster deposition can be obtained from the substrate signal attenuation. The average cluster size can be estimated by calculating the attenuation of this idealized overlayer, assuming that the Ag clusters are adequately represented by uniform hemispheres.[17] Such calculations indicate that the cluster radius increases with deposition from ~ 10 Å at 0.7 ML to ~ 27 Å at 7 ML. At higher coverage, the model is not applicable because of cluster overlap and the formation of an extended network. Evidence for this sintering is found in scanning and transmission electron microscopy studies of metal(clusters)/GaAs interfaces.[12]

From the above analysis it is apparent that the preformed clusters are likely to contain several hundreds of atoms, even for the equivalent of a single monolayer exposure. In order to investigate the onset of metallic character in these clusters, we have studied the valence-band evolution for Ag depositions from 0.01 to 21 ML. Representative results are shown in the right panel of

Fig. 3. The 0.1-ML spectrum reveals Ag d-band emission, but the d bands do not fully develop until the deposition of ~ 0.7 ML. For this Ag exposure the d-band spectral feature assumes its metalliclike full width at half maximum (FWHM) and its shape has converged to that of Ag. This reflects overlayer metallicity and agrees with our estimated cluster radius of 10 Å at 0.7 ML (roughly 130 atoms per cluster). At higher Ag dosages, the metallicity is more apparent as the substrate valence-band emission is attenuated and the Fermi-level cutoff in the sp states becomes visible. These observations regarding overlayer metallicity will be especially important in the forthcoming discussion of E_F movement for metal(clusters)-InP(110) interfaces.

Finally, it is interesting to compare the Ag(clusters)/InP(110) interface morphology to that of interfaces formed by Ag atom deposition at 60 and 300 K. Intriguingly, as presented in Fig. 4, atom deposition at 300 K and cluster deposition yield the same substrate signal attenuation rate ($1/e$ length 10.5 ML). Furthermore, nearly identical substrate attenuation profiles are obtained for 300-K atom-by-atom deposition and cluster deposition of Ag on GaAs(110).[22] Whereas Ag clusters form spontaneously by atom migration and agglomeration on semiconductor surfaces at 300 K, deposition using Xe buffer layers involves cluster formation on and in the Xe matrix and their lowering to the surface when this layer is thermally desorbed. Coincidence of the substrate attenuations resulting from atom deposition at 300 K and preformed cluster deposition then indicates that a similar cluster size distribution is attained. A significant difference between these two procedures to form interfaces is that cluster deposition reduces substrate disruption and no evidence for the segregation of In atoms is found.

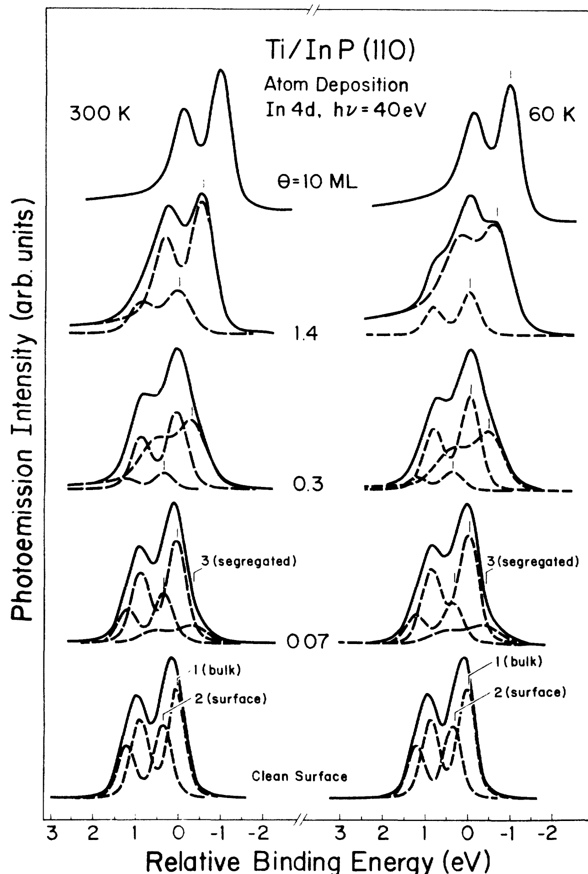

FIG. 5. Representative In $4d$ core-level EDC's and line-shape decompositions for Ti atom deposition at 300 and 60 K. Strong interfacial reaction releases In atoms whose emission results in the rapid development of component 3. Ti deposition disrupts ~ 4.4 ML of the substrate at both 300 and 60 K.

Ti/InP(110) atom deposition

In Fig. 5 we show representative In $4d$ EDC's for Ti/InP(110) interfaces formed at 300 K (left) and 60 K (right) to emphasize temperature-induced changes in interface morphology. Complete experiments involving samples with different bulk dopant concentrations were carried out at 60 and 300 K. Dopant concentration and dopant type do not affect interface morphology but there are interesting band-bending variations that are dependent on both parameters, as will be discussed in the next section. Line-shape decompositions for $\theta_{\text{Ti}}=0.1$ ML show a shoulder labeled 3 on the low-binding-energy side of the bulk substrate component at both temperatures. This shoulder is associated with In atoms released from the disrupted semiconductor surface. Interfacial reaction that leads to substrate disruption and cation release replaces the surface layers of InP(110) with Ti-P bonding configurations and the surface-shifted component (2) disappears completely by $\theta_{\text{Ti}}=1$ ML. For coverages below 0.3 ML there is little difference in the 300- and 60-K spectral line shape, and this again demonstrates that reaction is independent of temperature.

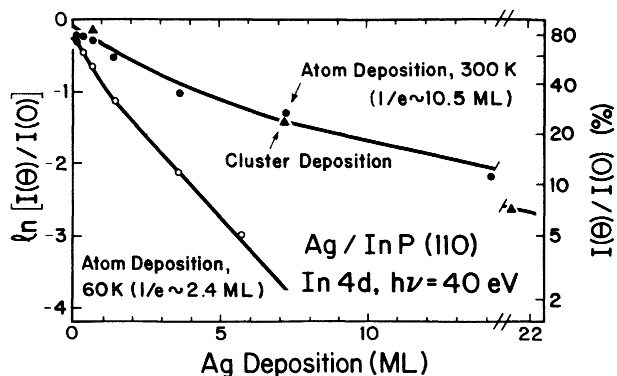

FIG. 4. Comparison of the substrate In $4d$ core-level attenuations for Ag cluster deposition and atom depositions at 300 and 60 K. The identical attenuations for the cluster deposition and atom-by-atom deposition at 300 K suggest similar morphologies and cluster size distribution at these interfaces. Rapid signal decay reflects uniform substrate coverage due to reduced Ag atom mobility at 60 K.

Ti-P bond formation at the interface releases In atoms from the substrate, and these cations are expelled toward the free surface as regions of the reacted phase grow and coalesce.[18] As shown in Fig. 5, the released-In emission

intensity grows rapidly and exceeds that of the bulk substrate for $\theta_{Ti} \geq 0.3$ ML. Beyond 0.3 ML, the FWHM of component 3 decreases as the (heterogeneous) local environment of the liberated In atoms converges to a more uniform segregated phase at 300 K. At 60 K, reduced cation mobility again kinetically traps these expelled atoms in the thickening Ti film. Kinetic trapping of these released In atoms at 60 K in a heterogeneous environment causes the Gaussian FWHM to remain broad ($\sim$700 meV) for 0.3 ML $\leq \theta_{Ti} \leq 3$ ML. At higher coverage the width decreases rapidly and it is reduced to 440 meV by 10 ML, equaling that of the 300-K spectra.

Additional information regarding the local environment of the liberated cations is provided by their binding energy (for metal–III-V-compound interfaces in general, the relative binding energy of this component decreases with coverage[18,19]). For Ti/InP(110), the shift is less pronounced at 300 K than at 60 K, amounting to -0.37 and -0.47 eV at 0.3 ML and -0.70 and -0.96 eV at 3.5 ML for 300 and 60 K, respectively. While the reduction in FWHM can be attributed to the increasingly homogeneous environment of the segregated cations at 300 K, the shift to lower binding energy indicates that they become progressively dispersed at the Ti surface. Segregation is very limited at 60 K as the cations become kinetically trapped. This metastable trapping is reflected in the gradual shift to lower binding energy of the emission from these dissociated In atoms. This spectral feature is asymmetric at both 300 and 60 K and this reveals a metallic environment of released In atoms. The asymmetry parameter required for successful fits at high coverages was $\sim$0.12 for 300-K and $\sim$0.20 for 60-K interfaces. This difference, noticeable in Fig. 5, possibly reflects the more Ti-rich environment at 60 K.

In Fig. 6 we show logarithmic attenuation curves for Ti/InP(110) formed at 300 K (top) and 60 K (bottom). Vigorous Ti-P chemical reaction leads to rapid substrate attenuation for $\theta_{Ti} \leq 1.5$ ML. At higher coverages, the rate of attenuation is smaller [$1/e$ lengths of $\sim$2 ML (2.9 Å) at 300 K and $\sim$2.8 ML (4.1 Å) at 60 K]. The slightly higher substrate attenuation rate at 300 K possibly indicates that reaction proceeds more slowly after $\sim$1.5 ML at 300 K but is kinetically inhibited at 60 K. A simple calculation based on substrate attenuation profiles establishes that 1.5-ML Ti deposition leads to disruption of $\sim$4.4 ML of substrate at both 300 and 60 K.

Strong chemical reaction and cation release induce an abrupt increase in the segregated In component (3) for $\theta_{Ti} \leq 1.5$ ML regardless of temperature. At 60 K, the segregated component intensity then remains unchanged at $\sim$40% of the clean-surface emission until $\sim$3.6 ML and attenuates at the same rate as the substrate signal at higher coverages. The constant intensity between 1.5 and 3.6 ML and attenuation above 3.6 ML correlate well with the previously discussed variations in the Gaussian width of component 3 (constant large Gaussian width below $\sim$3 ML with sharpening thereafter). From this and the changes in the substrate In $4d$ emission, we can discern three distinct steps in the Ti/InP interface formation at 60 K. There are (1) initial disruption and cation release, (2) trapping of the released cations in the Ti matrix, and

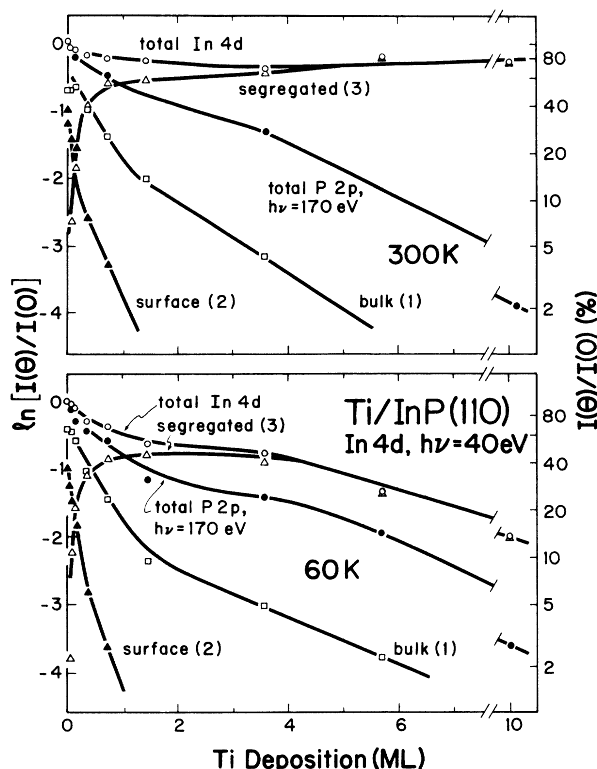

FIG. 6. Attenuation curves for the Ti/InP(110) interface at 300 K (top) and 60 K (bottom). At 300 K, strong In segregation results in continuous increase of the component-3 emission for $\theta_{Ti} \leq 10$ ML. The very slow subsequent decay of this component is due to the metastable trapping of these In atoms in Ti. At 60 K, In segregation is very limited above $\sim$4 ML of Ti. Total P $2p$ attenuations differ very little between 300 and 60 K and reveal pronounced chemical trapping of released P atoms at both temperatures.

(3) the final covering of the interface with very limited segregation of In atoms. For 300 K, however, thermodynamically preferred cation segregation results in substantially higher emission from the segregated In phase. Its intensity saturates between 6 and 10 ML at $\sim$80% of the clean-surface signal and attenuates very slowly for coverages above $\sim$10 ML, as shown in Ref. 18. Indeed, the emission from segregated In atoms equals $\sim$30% of the clean-surface In $4d$ signal even for 55-ML Ti coverage.

Figure 7 shows the P $2p$ core-level line-shape evolution for the Ti/InP interface formed at 60 K. The component-specific attenuation profiles for this interface are shown in the inset. Fitting of the clean-surface spectrum required two components, namely, substrate emission and a surface-shifted feature at -0.30 ± 0.03 eV. The S/B ratio for $h\nu = 140$ eV is $\sim$33%, corresponding to the photoelectron mean free path of $\sim$8 Å. Submonolayer Ti deposition resulted in enhanced emission at lower binding energy that is associated with surface disruption and Ti-P bond formation. This new feature (labeled 3) is degenerate with the surface-shifted component for $\theta_{Ti} \leq 0.1$ ML. At higher coverage it grows and shifts

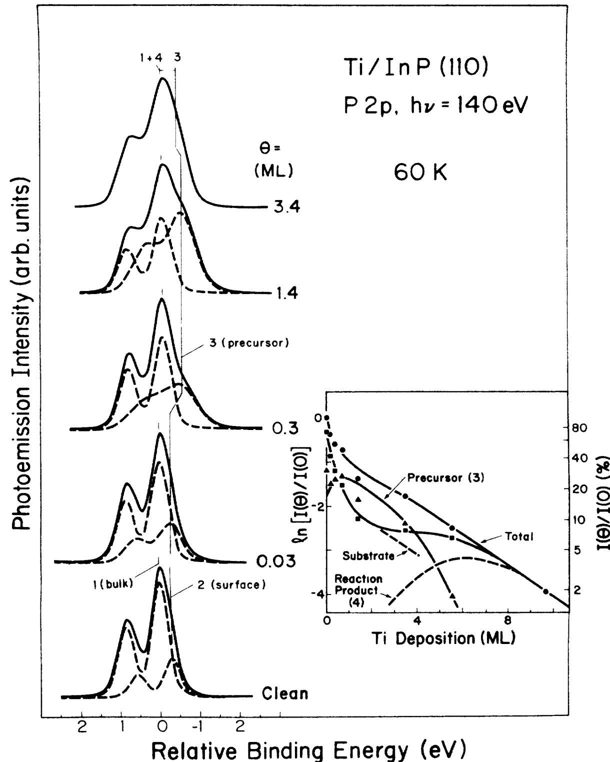

FIG. 7. Representative P 2p core-level EDC's and line-shape decompositions for Ti/InP(110) formed at 60 K. Components 1 and 2 correspond to the P atoms in the semiconductor bulk and at the surface, respectively. Component 3 reflects the metastable (precursor) Ti-P bonding configuration which is at higher coverage replaced by fully developed Ti-rich phosphide evidenced in component 4. Components 1 and 4 are degenerate in energy and their component specific attenuations shown in the inset were obtained using the In 4d substrate attenuation.

to lower binding energy so that a distinct shoulder in the P 2p emission is observed at 0.3 ML. For $\theta_{\text{Ti}} \geq 1.4$ ML, the intensity of this component decreases with a rate exceeding that of the total P 2p emission. Likewise, the binding energy of this component shifts back toward that of the substrate. This indicates that component 3 is a precursor to the more stable Ti-P phase in the sense that its bonding configuration is not yet completely defined. The P 2p binding energy of the fully developed Ti-P configuration is degenerate with that of bulk InP, but its existence is clear from the attenuation results shown in the inset. In particular, the extrapolated substrate signal attenuation (dashed line) is used to remove the substrate contribution from the completely reacted component (4). This procedure then shows that the component (4) is the only remaining feature in the spectrum for $\theta_{\text{Ti}} \geq 7$ ML, and its emission is attenuated exponentially at higher coverage. The total P 2p emission attenuation at 300 K is identical to that at 60 K (Fig. 6) and this reflects temperature-independent interfacial chemical reaction and anion retention in the reacted region. Finally, the P 2p line-shape evolution at 300 K is the same as that at 60 K, again emphasizing that adatom-substrate reaction is not altered and that the interface region is dominated by Ti-P bonding at both 60 and 300 K.

Identical results regarding the temperature effects on substrate disruption and interfacial chemical reaction were observed for Al, Co, and Ti overlayers on GaAs(110) as well as Ag, Au, and Ga overlayers on InP(110).[10-12] For each of those interfaces, the absolute amount of substrate disruption is equal at 60 and 300 K. Changes in temperature significantly affect released atom distributions and, as discussed next, the Fermi-level movement at these interfaces.

FERMI-LEVEL EVOLUTION

Ag and Ti atom deposition at 60 and 300 K

In the following we discuss E_F evolution for Ag and Ti overlayers on cleaved InP(110) formed by atom depositions at 60 and 300 K and by the deposition of preformed Ag clusters. We also investigate effects of substrate dopant concentration on surface Fermi-level position for depositions below ~ 2 ML.

Figure 8 shows the movement of E_F at the InP(110) surface. The solid lines represent atom deposition and the dashed lines for Ag/InP show the results for Ag cluster deposition. Energies are referenced to the CBM for n-type InP substrates and the VBM for p-type InP. Because of the different energy references for n- and p-type samples, we emphasize that the separation between the CBM and the VBM in Fig. 8 is *not* equal to the InP band gap (1.35 eV at 300 K and 1.42 eV at 60 K). The results in Fig. 8 were obtained on heavily doped (HD) substrates with $N_D = N_A \sim 2.5 \times 10^{18}$ cm^{-3}.

As shown in Fig. 8, E_F moves gradually for n-type InP at 300 K and establishes barrier heights of 0.72 ± 0.03 eV for $\theta_{\text{Ag}} = 10$ ML and 0.57 ± 0.03 eV for $\theta_{\text{Ti}} = 3.5$ ML. The Ti/(p-type InP) data show rapid E_F movement at low coverage and a broad plateau between ~ 0.1 and ~ 1 ML with a subsequent shift back toward the VBM (0.72 eV above the VBM at ~ 4 ML and possible further movement at higher coverage to a final barrier height). This interesting Fermi-level behavior for p-type substrates is analogous to that observed for 300-K Au atom deposition on InP(110).[10] For Ag/(p-type InP), band bending increases more gradually and saturates 0.64 ± 0.03 eV from the VBM above ~ 1 ML. The absence of an overshoot is probably related to the widely scattered distribution of Ag clusters in the low-coverage regime, and this could result in inhomogeneous surface band bending. Significantly, these Ag/InP(110) results indicate an average final pinning position for n- and p-type substrates of 0.67 ± 0.03 eV above the VBM for atom deposition at 300 K. They disagree with the 300-K results of Cao *et al.*,[3] which indicate E_F pinning at the antisite defect energy 0.95 eV above the VBM.

The 60-K results for Ag and Ti atom depositions on n-type InP(110) show a characteristic step in E_F position that is followed by the convergence to the 300-K positions at high coverage. For Ag/(n-type InP) the step is rather poorly defined (movement from 0.30 eV below the

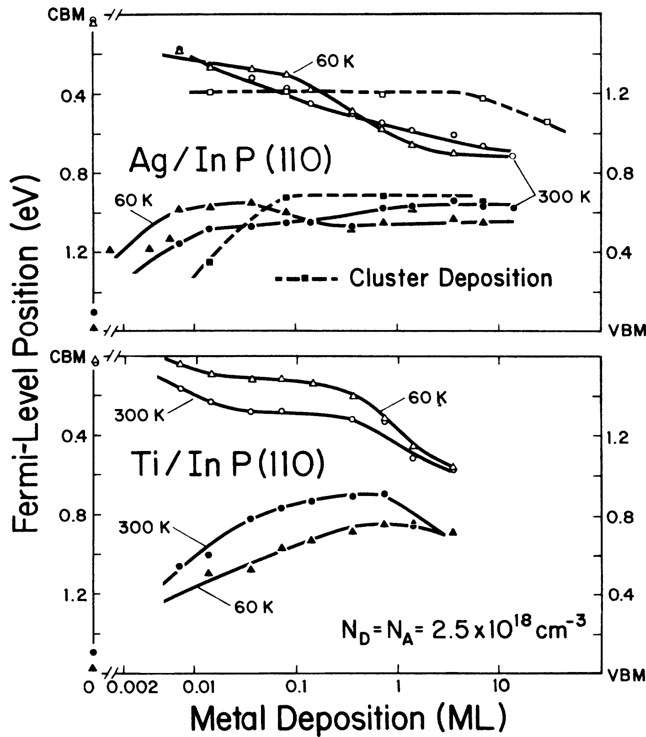

FIG. 8. Temperature-dependent E_F movement as a function of Ag (top) and Ti (bottom) depositions on heavily doped InP(110). Open and closed symbols correspond to the *n*- and *p*-type substrate, respectively. Ag cluster deposition results are represented by squares and dashed lines. Fermi level for *n*-type (*p*-type) InP is referenced to the CBM (VBM) and the respective energy scales are shown on the left and on the right axes of the diagram. Energy separation between the lower and the upper axes is not equal to the band gap. Ag and Ti results for 300 and 60 K show the same high-coverage E_F positions. Ag cluster deposition results in coverage-insensitive E_F pinning positions 0.40 eV beneath the CBM for *n*-type InP and 0.70 eV above the VBM for *p*-type InP.

CBM at ~ 0.1 ML to 0.70 eV at ~ 3 ML). This energy at 3 ML is within 20 meV of the 300-K position and does not change with further deposition. This result agrees with the 80-K results of Cao *et al.*[3] Ti/(*n*-type InP) results at 60 K show a E_F position ~ 0.10 eV below the CBM for 0.01 ML $\leq \theta_{Ti} \leq 0.1$ ML and rapid E_F movement above 0.1 ML. At the highest coverage for which the substrate signal could be followed (3.5 ML), E_F was 0.57 ± 0.03 eV below the CBM, again at the same position observed at 300 K. The 60-K results for Ag/(*p*-type InP) show a ~ 100-meV overshoot at ~ 0.05 ML and E_F stabilization 0.55 ± 0.03 eV above the VBM for $\theta_{Ag} \geq 0.2$ ML. This overshoot is less pronounced in E_F movement for Ti/(*p*-type InP) formed at 60 K but the agreement between 60 and 300 K is again excellent for θ_{Ti} above ~ 1 ML.

A recent series of studies of temperature and dopant-concentration effects on E_F movement at metal/GaAs(110) interfaces has provided new insight into the interaction of semiconductor surfaces with adatoms.[5-7,22] They have shown that substrate disruption is independent of sample temperature but that temperature cycling between 20 and 300 K induces (reversible) changes in band bending. The dopant concentration of the substrate is a particularly important parameter, and we consider its effect for Ag and Ti/[*n*-type InP(110)] in the following.

Figure 9 shows temperature-dependent E_F movement for Ag and Ti overlayers on *n*-type InP(110) lightly doped (LD) at 4×10^{17} cm^{-3}. The resemblance between Ag and Ti results for these lightly doped samples is closer than for heavily doped samples (Fig. 8) because of the reduction in band bending for submonolayer coverages at 60 K. For Ag/InP at 300 K, the Fermi-level movement exhibits a vestigial step at approximately the same coverage as at 60 K (1 to 3 ML). Significantly, this step is absent from the HD results for Ag/InP at 300 K. For Ti/InP, the step appears for both dopant concentrations at 300 K. This metallization-induced step is more pronounced at 60 K as band bending at submonolayer coverages is reduced with temperature. As noted earlier, the high-coverage pinning positions are largely insensitive to temperature, and comparison of the HD results (Fig. 8) and LD results (Fig. 9) indicates that the final barrier heights are also independent of substrate dopant concentration. This comparison also shows that the step is more pronounced for LD samples since the low-coverage band bending is significantly smaller than for HD samples at 60 K. More specifically, the low-coverage Fermi-level plateau is ~ 100 meV beneath the CBM for Ti atom deposition onto samples doped to 2.5×10^{18} cm^{-3} and ~ 50 meV for 4×10^{17} cm^{-3}. For Ag overlayers, more heavily doped samples do not exhibit a clear plateau, but the plateau is ~ 260 meV beneath the CBM for 0.01 ML $\leq \theta_{Ag} \leq 0.6$ ML for lightly doped samples.

The temperature and dopant-concentration effects for submonolayer deposition can be understood in terms of the coupling of the surface and bulk, as introduced by Aldao *et al.*[7] and modified by Hecht[8] and Aldao *et al.*[9] In Ref. 7, the coupling was associated with charge exchange under a dynamic equilibrium configuration. Detailed analysis of the dependence of the apparent E_F position on photon or electron flux showed that the system should be better considered as nonequilibrium, as Hecht suggested.[9] In this case, a surface photovoltage (SPV) is established by the photon beam as electrons and holes are separated within the depletion region. For measurements at 300 K or with high dopant concentration, the SPV is small or negligible for the flux values of photoemission, but the effect is larger at low temperature or low dopant concentration. In effect, the SPV serves to flatten the bands, and the apparent E_F position remains close to the CBM or VBM. The ability of the nonequilibrium SPV effect to describe the low-coverage metal-GaAs(110) results indicates that such effects are dominant. The applicability of such a description to InP(110) is then straightforward.

In summary, Fermi-level movement for Ag/InP(110) and Ti/InP(110) exhibits temperature- and dopant-concentration effects that can be explained within the framework of a surface that is uncoupled from the bulk.

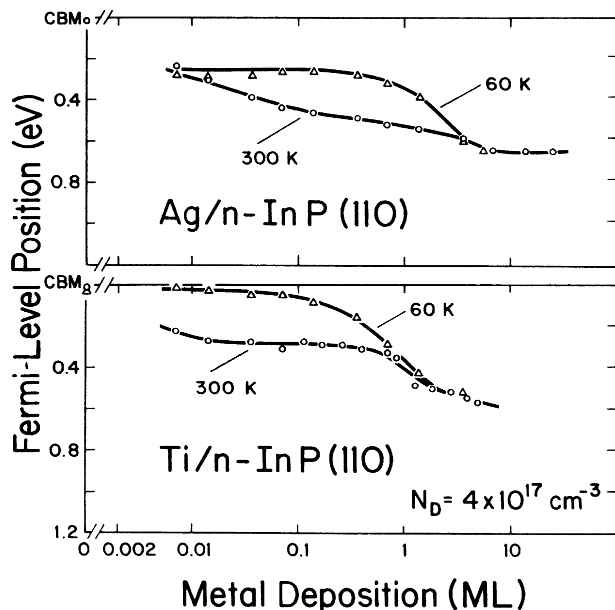

FIG. 9. E_F position as a function of Ag (top) and Ti (bottom) atom deposition on lightly doped n-type InP(110). Comparison with the results obtained on heavily doped substrates in Fig. 8 show identical high-coverage E_F pinning positions. The submonolayer coverage band bending for 60 K is significantly reduced and the metallization step is more pronounced compared to the HD samples.

In the isolated-adatom regime, the predicted barrier heights scale with system temperature and dopant concentration. Indeed, for both substrate dopant concentrations, the Ag/InP and Ti/InP results indicate higher band bending at 300 K than at 60 K. At 60 K, the model predicts an increase in low-coverage band bending with increasing dopant concentration. This change is less pronounced than the temperature effects because of the relatively small range of the dopant concentrations available for this study of InP (the HD and LD sample dopant concentration varies by a factor of about 5). Nevertheless, the effect observed for both Ti and Ag overlayers on InP(110) agrees well with the results for Ti, Co, and Ag overlayers on GaAs(110) substrates where it was possible to vary the dopant concentration by two orders of magnitude.[6,7]

Ag cluster deposition

The deposition of preformed metal clusters results in a metal-semiconductor interface with unique morphological and electrical characteristics. In the following, we show how the interface morphology correlates with E_F movement for these interfaces. This E_F movement for Ag(clusters)/InP(110) for n- and p-type substrates is shown by dashed lines in the top panel of Fig. 8. Each datum point on these curves was obtained from a freshly cleaved and characterized InP(110) surface after condensation of a 30-Å Xe buffer layer, Ag deposition on top of it, and thermal desorption of the Xe layer. The band bending and interface morphology were then assessed by analysis of the bulk and surface-sensitive substrate core levels. For n-type InP, E_F remains at 0.40 ± 0.03 eV beneath the CBM for Ag dosages between ~0.015 and 7 ML, but it drops to 0.53 eV for 20 ML nominal deposition. This increase in band bending for 20 ML is presently not well understood but it may reflect the effect of cluster coalescence at high coverage. This layer would form a nearly contiguous overlayer with morphology and contact properties similar to those for interfaces formed by atom deposition. In that context, the drop into the gap could signal the convergence to the E_F position achieved at high coverage by atom deposition. The E_F positions for nominal depositions below 20 ML are identical to those observed for the Au(clusters)/InP(110) interface; the invariance with coverage is characteristic of E_F behavior for a number of cluster overlayers on GaAs(110).[12,17] Such coverage independence and unique pinning positions are in sharp contrast with the atom deposition experiments. The results cannot be interpreted with existing models of Schottky-barrier formation.

A slightly different evolution of the surface E_F is observed for Ag(clusters)/[p-type InP(110)] of matched dopant concentration (2.5×10^{18} cm^{-3}). Data show that 0.015-ML deposition results in a E_F position 0.36 eV above the VBM. For higher nominal dosages, it is coverage independent and located 0.68 eV above the VBM. The reduced band bending for 0.015 ML compared to higher Ag exposition is possibly due to inhomogeneous surface band bending. Cluster deposition studies on GaAs(110) substrates with comparable substrate dopant concentration have shown that electrostatic effects can significantly reduce the band bending if the cluster separation is larger than the depletion region.[12] It is then conceivable that nonuniform band bending will result in a reduction of the average surface potential for very small nominal deposition where the expected cluster separation is large.

The final Fermi-level positions for Ag(clusters)/InP(110) are different for n- and p-type substrates. This can also be observed for metal(clusters)/GaAs(110) systems, and it reflects a difference in the mechanism(s) determining cluster-induced E_F pinning for n- and p-type doped semiconductors. It rules out MIGS as the dominant pinning mechanism since MIGS are expected to pin E_F at the same position in the gap for both n-type and p-type InP (~0.76 eV above the VBM). This is particularly interesting since, as discussed previously, overlayer metallicity for interfaces formed by cluster deposition is established for nominal depositions exceeding ~1 ML (see valence band spectra in Fig. 3). Moreover, these cluster deposition results cannot be reconciled with the defect pinning mechanism either since such defects would be predicted to pin E_F 0.95 eV above the InP VBM, a value that is far from the value of 0.68 eV obtained for Ag(clusters)/(p-type InP). The applicability of defect models to cluster interfaces is also questionable since cluster deposition results in much less substrate disturbance than atom deposition.

We postulate that surface Fermi-level movement at interfaces formed by cluster deposition is induced by surface unrelaxation and nondisruptive modification under-

neath and around the clusters. This is responsible for the reduction of the surface-shifted component intensity (Fig. 3). Since surface relaxation for cleaved GaAs(110) and InP(110) surfaces sweeps the intrinsic surface states out of the gap, these states can be reintroduced as the surface geometry is modified by metal clusters. Their existence has been verified by scanning tunneling microscopy (STM) studies which imaged the distribution of states near clusters of Sb on GaAs(110).[23] Unfortunately, lattice mismatch between the cluster and the substrate can modify the energy position of these intrinsic surface states and their energies cannot be readily predicted. The fact that the cluster-specific band bending is higher for p- than for n-type substrates of matched doping is, however, in good agreement with the intrinsic surface level calculations by Chadi.[24] This emphasizes the role of surface unrelaxation in Fermi-level pinning for metal-semiconductor interfaces formed by cluster deposition.

CONCLUSIONS

This paper has shown that Ag- and Ti-atom deposition on InP(110) results in significantly different morphologies and amounts of substrate disruption. Ti atoms react with substrate anions and In atoms liberated from the substrate segregate to the free surface. These cations are able to diffuse to the top of the Ti overlayer at 300 K but they are kinetically trapped at the interface at 60 K. Silver atoms cluster spontaneously on InP(110) at 300 K, but cover the substrate uniformly at 60 K because of reduced surface mobility. These Ag atoms induce limited substrate disruption and substrate atoms are released into the overlayer at both 300 and 60 K. Again, cation segregation is pronounced at 300 K but is thermally inhibited at 60 K. Despite differences in Ag/InP and Ti/InP interfacial morphologies, there are very similar temperature- and dopant-concentration-dependent Fermi-level movements. These results are in very good agreement with the changes in E_F position for numerous metal/GaAs(110) systems because of the inability of the surface to couple with the bulk. Ag(clusters)/InP(110) interfaces show no sign of substrate disruption and produce unique, nearly coverage-independent E_F positions. For these interfaces, E_F pinning is likely to be caused by intrinsic semiconductor surface states reintroduced into the gap by surface modification beneath and around the clusters.

ACKNOWLEDGMENTS

This work was supported by the U.S. Office of Naval Research under Contracts No. N00014-86-K-0427 and No. N00014-87-K-0029. The assistance of the staff of the National Science Foundation (NSF) -supported University of Wisconsin storage ring at Stoughton, WI, is gratefully acknowledged.

[1]See, for example, E. H. Rhoderick and R. H. Williams, in *Metal-Semiconductor Contacts*, 2nd ed. (Clarendon, Oxford, 1988); J. L. Freeouf, Surf. Sci. **132**, 233 (1983); L. J. Brillson, Surf. Sci. Rep. **2**, 123 (1982). A recent overview is given by J. H. Weaver, A New Era in Materials Science, edited by J. R. Chelikowsky and A. Franciosi (Springer-Verlag, Berlin, in press), Chap. 7.

[2]K. Stiles, A. Kahn, D. G. Kilday, and G. Margaritondo, J. Vac. Sci. Technol. B **5**, 987 (1987); K. Stiles, S. F. Horng, A. Kahn, J. McKinley, D. G. Kilday, and G. Margaritondo, *ibid.* **6**, 1392 (1988).

[3]W. E. Spicer, R. Cao, K. Miyano, C. McCants, T. T. Chiang, C. J. Spindt, N. Newman, T. Kendelewicz, I. Lindau, E. Weber, and Z. Liliental-Weber, in *Metallization and Metal-Semiconductor Interfaces*, Vol. 195 of *NATO Advanced Study Institute, Series B*, edited by I. P. Batra (Plenum, New York, 1989); R. Cao, K. Miyano, T. Kendelewicz, I. Lindau, and W. E. Spicer, Phys. Rev. B **39**, 11 146 (1989).

[4]V. Heine, Phys. Rev. A **138**, 1689 (1965); S. G. Louie, J. R. Chelikowsky, and M. L. Cohen, Phys. Rev. B **15**, 2154 (1977); J. Tersoff, Phys. Rev. Lett. **52**, 465 (1984); J. Vac. Sci. Technol. B **3**, 1157 (1985).

[5]C. M. Aldao, S. G. Anderson, C. Capasso, G. D. Waddill, I. M. Vitomirov, and J. H. Weaver, Phys. Rev. B **39**, 12 977 (1989); S. G. Anderson, C. M. Aldao, G. D. Waddill, I. M. Vitomirov, C. Capasso, and J. H. Weaver, Appl. Phys. Lett. **55**, 2547 (1989).

[6]I. M. Vitomirov, G. D. Waddill, C. M. Aldao, S. G. Anderson, C. Capasso, and J. H. Weaver, Phys. Rev. B **40**, 3483 (1989).

[7]C. M. Aldao, I. M. Vitomirov, G. D. Waddill, S. G. Anderson, and J. H. Weaver, Phys. Rev. B **41**, 2800 (1990).

[8]M. Hecht, Phys. Rev. B (to be published).

[9]C. M. Aldao, G. D. Waddill, P. J. Benning, C. Capasso, and J. H. Weaver, in Phys. Rev. B **41**, 6092 (1990), discussed surface photovoltaic effects and their dependence on temperature dopant concentration and coverage.

[10]G. D. Waddill, C. M. Aldao, I. M. Vitomirov, Y. Gao, and J. H. Weaver, J. Vac. Sci. Technol. A **7**, 865 (1989) for temperature-dependent Au/InP(110) evolution. Line-shape-analysis procedures are discussed in detail in J. J. Joyce, M. del Giudice, and J. H. Weaver, J. Electron Spectrosc. Relat. Phenom. **49**, 31 (1989).

[11]I. M. Vitomirov, C. M. Aldao, M. Schabel, G. D. Waddill, S. G. Anderson, and J. H. Weaver, J. Vac. Sci. Technol. A **7**, 758 (1989) for Ga/InP(110) results.

[12]G. D. Waddill, I. M. Vitomirov, C. M. Aldao, and J. H. Weaver, Phys. Rev. Lett. **62**, 1568 (1989); G. D. Waddill, I. M. Vitomirov, C. M. Aldao, S. G. Anderson, C. Capasso, J. H. Weaver, and Z. Liliental-Weber, Phys. Rev. B (to be published); C. M. Aldao, G. D. Waddill, S. G. Anderson, and J. H. Weaver, Phys. Rev. B **40**, 2932 (1989).

[13]R. Ludeke, T.-C. Chiang, and T. Miller, J. Vac. Sci. Technol. B **1**, 418 (1983); K. K. Chin, S. H. Pan, D. Mo, P. Mahowald, N. Newman, I. Lindau, and W. E. Spicer, Phys. Rev. B **32**, 918 (1985).

[14]K. Stiles and A. Kahn, Phys. Rev. Lett. **60**, 440 (1988).

[15]B. M. Trafas, F. Xu, M. Vos, C. M. Aldao, and J. H. Weaver, Phys. Rev. B **40**, 4022 (1989) for metal overlayers on

GaP(110).

[16]M. Vos, F. Xu, S. G. Anderson, J. H. Weaver, and H. Cheng, Phys. Rev. B **39**, 10 744 (1989); M. Vos, C. M. Aldao, D. J. W. Aastuen, and J. H. Weaver, Phys. Rev. B **41**, 991 (1990) for metal overlayers and for Ag-ion and neutral-atom growth on ZnSe(110).

[17]C. M. Aldao, I. M. Vitomirov, G. D. Waddill, and J. H. Weaver, Appl. Phys. Lett. **53**, 2647 (1988).

[18]C. M. Aldao, I. M. Vitomirov, F. Xu, and J. H. Weaver, Phys. Rev. B **37**, 6019 (1988); I. M. Vitomirov, F. Xu, C. M. Aldao, and J. H. Weaver, J. Vac. Sci. Technol. A **6**, 1563 (1988).

[19]B. M. Trafas, I. M. Vitomirov, C. M. Aldao, Y. Gao, F. Xu, J. H. Weaver, and D. L. Partin, Phys. Rev. B **39**, 3265 (1989).

[20]A. K. Niessen, F. R. de Boer, R. Boom, P. F. de Chatel, W. C. M. Mattens, and A. R. Miedema, Comput. Compl. Phase Diagr. Thermochem. (CALPHAD) **7**, 51 (1983).

[21]J. H. Weaver, Z. Lin, and F. Xu, in Surface Segregation and Related Phenomena, edited by P. A. Dowben and A. Miller (CRC, Boca Raton, in press), Chap. 10.

[22]G. D. Waddill, I. M. Vitomirov, C. M. Aldao, S. G. Anderson, C. Capasso, and J. H. Weaver, J. Vac. Sci. Technol. B **7**, 950 (1989).

[23]R. M. Feenstra and P. Mårtensson, Phys. Rev. Lett. **61**, 447 (1988).

[24]D. J. Chadi, Phys. Rev. B **18**, 1800 (1978).